Overview of MHD Computation for Magnetic Confinement Fusion

Carl Sovinec

University of Wisconsin-Madison

2014 MHD Power Generation Workshop

Arlington, Virginia October 1-2, 2014

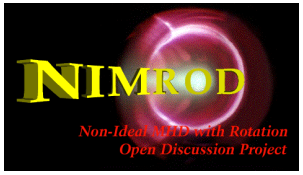

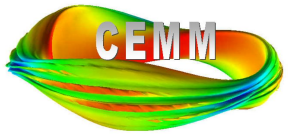

MFE MHD computations include magnetic-island evolution and relaxation from magnetic tearing.

- Magnetic islands alter the confining topology, providing a conduit for enhanced energy transport.
- They also impede plasma flow.

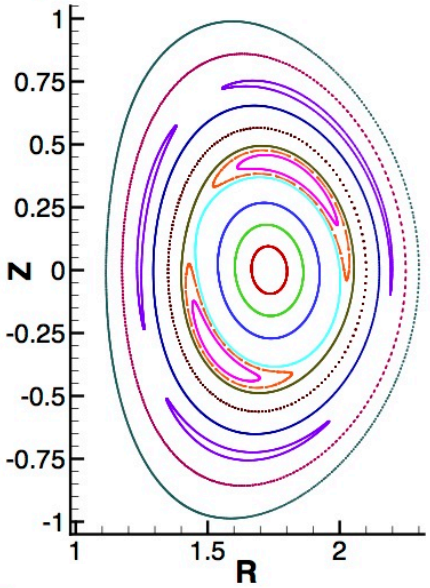

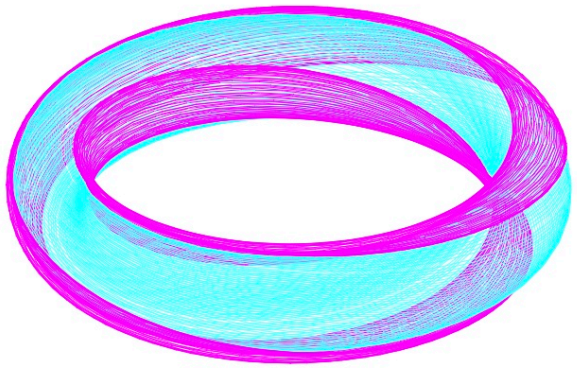

Field-line traces and puncture plot of a 3D MHD tokamak computation.

- Transient 3D MHD activity leads to spheromak formation.

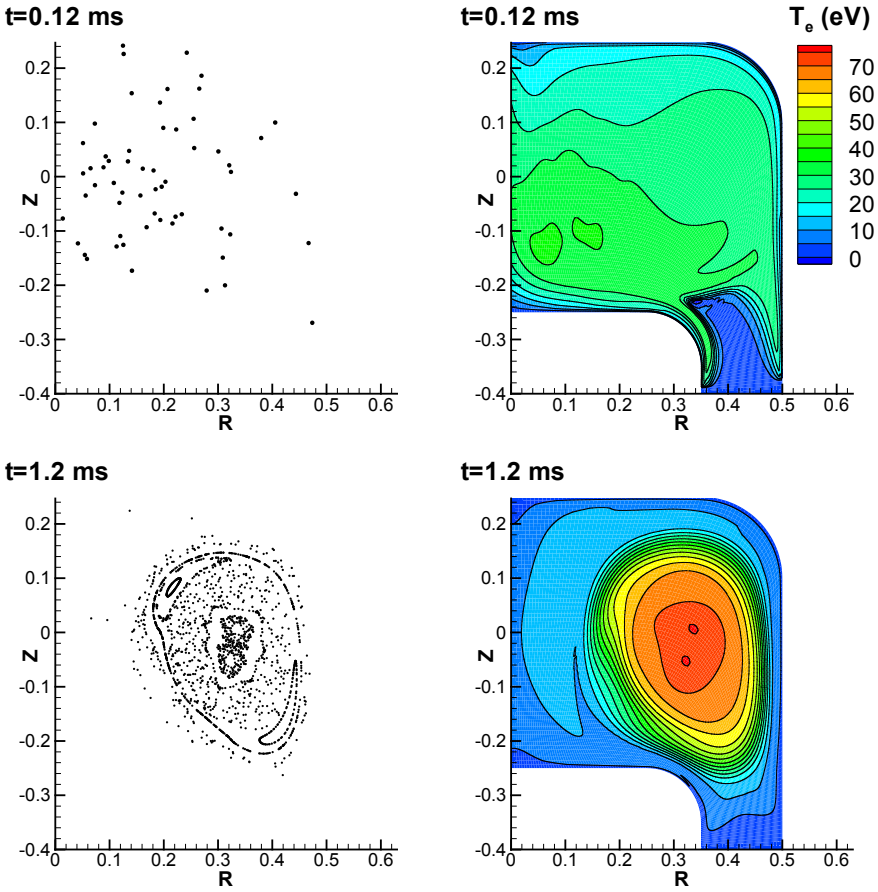

Spheromak simulation results on **B**-topology and temp. for SSPX [PRL **94**].

Applications to edge-localized modes and disruptions show plasma-surface distortion and movement.

- ELMs concentrate heat flux temporally and alter the deposition location.

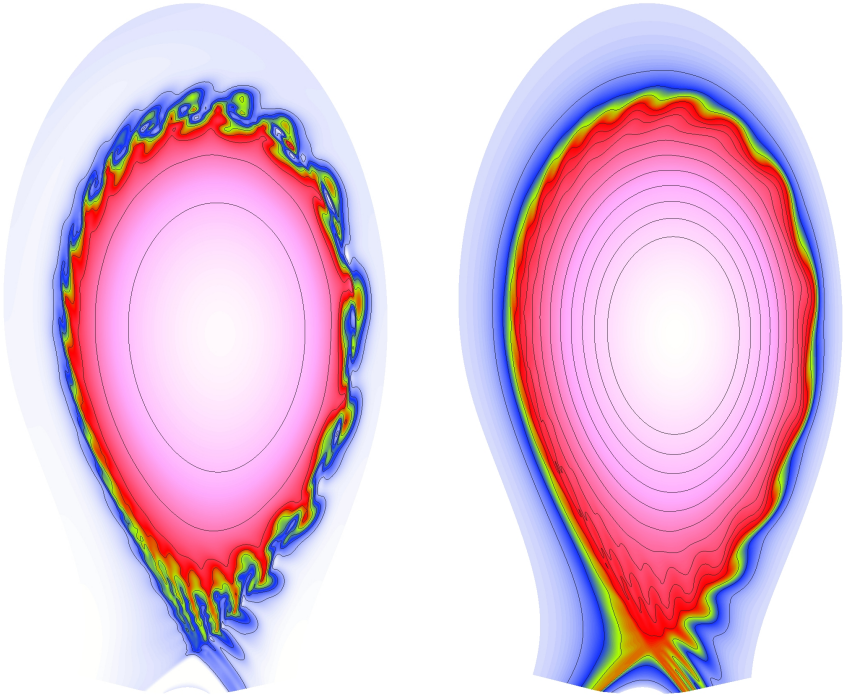

Density (left) and temp. (right) from a JOREK simulation by Huysmans, et al., PPCF **51**, 124012 (2009).

- Vertical displacement instability moves the plasma torus into the first wall.

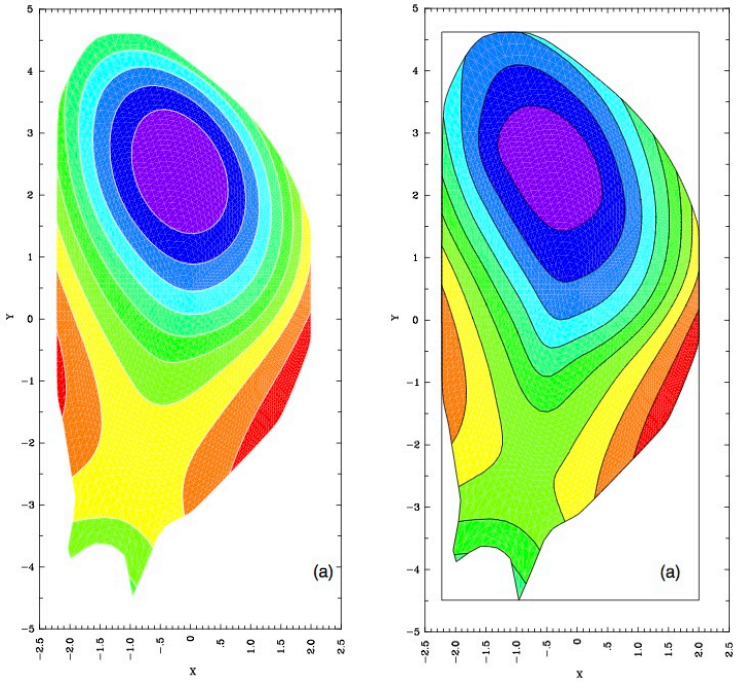

Poloidal flux contours from an M3D simulation by Strauss et al., PoP **17**, 082505 (2010).

Simulations of MFE macroscopic dynamics are based on single- and two-fluid plasma models.

$$\frac{\partial n}{\partial t} + \nabla \cdot (n\mathbf{V}) = \nabla \cdot \left(D_n \nabla n - D_h \nabla \nabla^2 n \right)$$

continuity with diffusive numerical fluxes

$$mn\left(\frac{\partial}{\partial t} + \mathbf{V} \cdot \nabla \right) \mathbf{V} = \mathbf{J} \times \mathbf{B} - \nabla \sum_{\alpha} n T_{\alpha} - \nabla \cdot \underline{\Pi}$$

flow evolution

$$\frac{3}{2} n \left(\frac{\partial}{\partial t} + \mathbf{V}_{\alpha} \cdot \nabla \right) T_{\alpha} = -n T_{\alpha} \nabla \cdot \mathbf{V}_{\alpha} - \nabla \cdot \underline{\mathbf{q}_{\alpha}} + Q_{\alpha}$$

temperature evolution

$$\frac{\partial \mathbf{B}}{\partial t} = -\nabla \times \left[\eta \mathbf{J} - \mathbf{V} \times \mathbf{B} + \underline{\frac{1}{ne} \mathbf{J} \times \mathbf{B} - \frac{T_e}{ne} \nabla n + \frac{m_e}{ne^2} \frac{\partial}{\partial t} \mathbf{J}} \right]$$

Faraday's / Ohm's law

$$\mu_0 \mathbf{J} = \nabla \times \mathbf{B}$$

low-ω Ampere's law

- Large resistivity keeps current density negligible outside the plasma part of the central region, and small mass density maintains accurate inertia.
- Two-fluid contributions appear in underlined terms.

The closure for stress ($\underline{\Pi}$) can be a combination of Braginskii ion gyroviscosity and anisotropic viscous stress.

$$\underline{\Pi}_{gv} = \frac{m_i p_i}{4eB}\left[\hat{\mathbf{b}}\times\underline{\mathbf{W}}\cdot\left(\underline{\mathbf{I}}+3\hat{\mathbf{b}}\hat{\mathbf{b}}\right)-\left(\underline{\mathbf{I}}+3\hat{\mathbf{b}}\hat{\mathbf{b}}\right)\cdot\underline{\mathbf{W}}\times\hat{\mathbf{b}}\right], \quad \left(\underline{\mathbf{W}} \equiv \nabla\mathbf{V}+\nabla\mathbf{V}^{\mathrm{T}}-\frac{2}{3}\underline{\mathbf{I}}\nabla\cdot\mathbf{V}\right)$$

$$\underline{\Pi}_{\perp} \sim -\frac{3p_i m_i^2}{10e^2B^2\tau_i}\underline{\mathbf{W}}$$

$$\underline{\Pi}_{\parallel} = \frac{p_i\tau_i}{2}\left(\hat{\mathbf{b}}\cdot\underline{\mathbf{W}}\cdot\hat{\mathbf{b}}\right)\left(\underline{\mathbf{I}}-3\hat{\mathbf{b}}\hat{\mathbf{b}}\right)$$

Similarly, the closure for conductive heat-flux density for each species ($\mathbf{q}_\alpha$) can include different effects.

$$\mathbf{q}_\alpha = -n\left[\chi_{\parallel\alpha}\hat{\mathbf{b}}\hat{\mathbf{b}}+\chi_{\perp\alpha}\left(\mathbf{I}-\hat{\mathbf{b}}\hat{\mathbf{b}}\right)\right]\cdot\nabla T_\alpha+\frac{5}{2}\left(\frac{p_\alpha}{q_\alpha B}\right)\hat{\mathbf{b}}\times\nabla T_\alpha$$

- The above relations are for large magnetization ($\Omega_\alpha\tau_\alpha$>>1).
- MFE computations often use simplified closure relations.

Variation of magnetization in time and space has been used in at least one application.

- Non-inductive startup from localized current injection is studied experimentally in the Pegasus Toroidal Experiment [Eidietis et al., JoFE **26**, 43 (2007), Battaglia, et al., NF **51**, 073029 (2011)].
- Simulations with the NIMROD code model electrical current development and relaxation [O'Bryan and Sovinec, PoP **19**, 080701 (2012)].

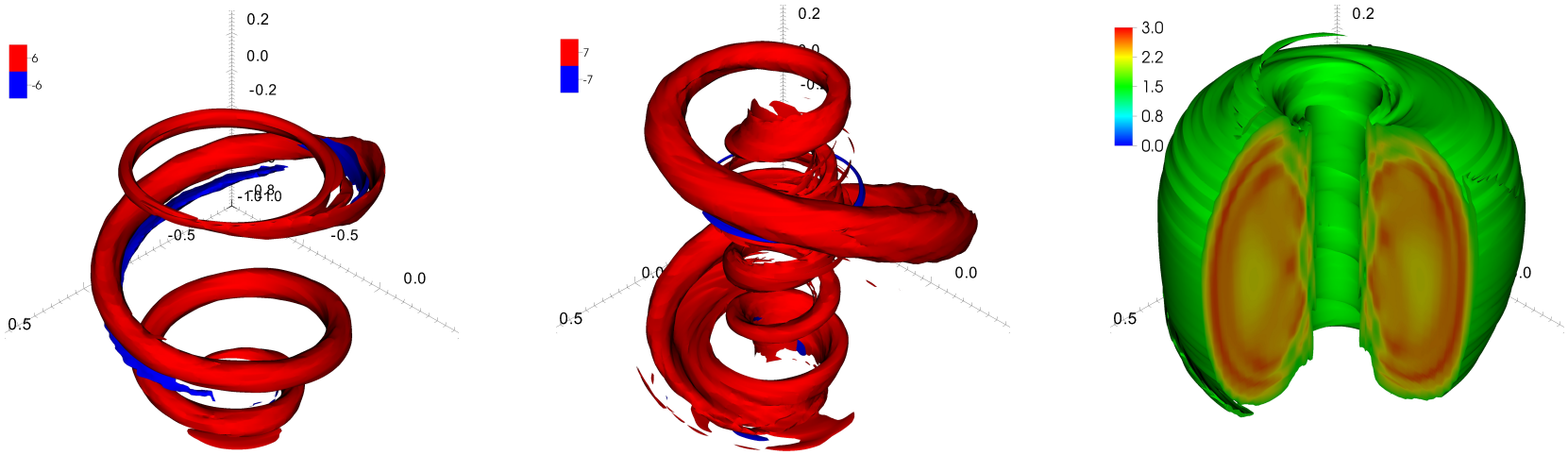

Isosurfaces of normalized parallel current density ($J_{||}/B$) for early (left) and late (center) in the driven phase, and after cessation of localized injection (right).

- Regions between filaments are unmagnetized early in time, and variable magnetized effects on heat-flux density are modeled.
- Variable magnetization for ion viscous stress has been implemented.

Modeling of plasma/neutral dynamics is important for small experiments and for edge conditions.

- A fluid model for interacting plasma and neutral species is developed in Meier and Shumlak, PoP **19**, 0872508 (2012).
  - Collisional effects include scattering and reaction (ionization, recombination, charge exchange).
  - Neutral and plasma species are coupled through source/sink terms in the continuity, momentum density, and energy equations.
- The model has been implemented in the HiFi code [Glasser and Tang, CPC **164**, 237 (2004); Lukin, PhD thesis, Princeton Univ. (2008)].

Simulation result for the Electrodeless Lorentz Force thruster using HiFi with dynamic neutral modeling. [Meier, PhD thesis, Univ. of Washington (2011).]

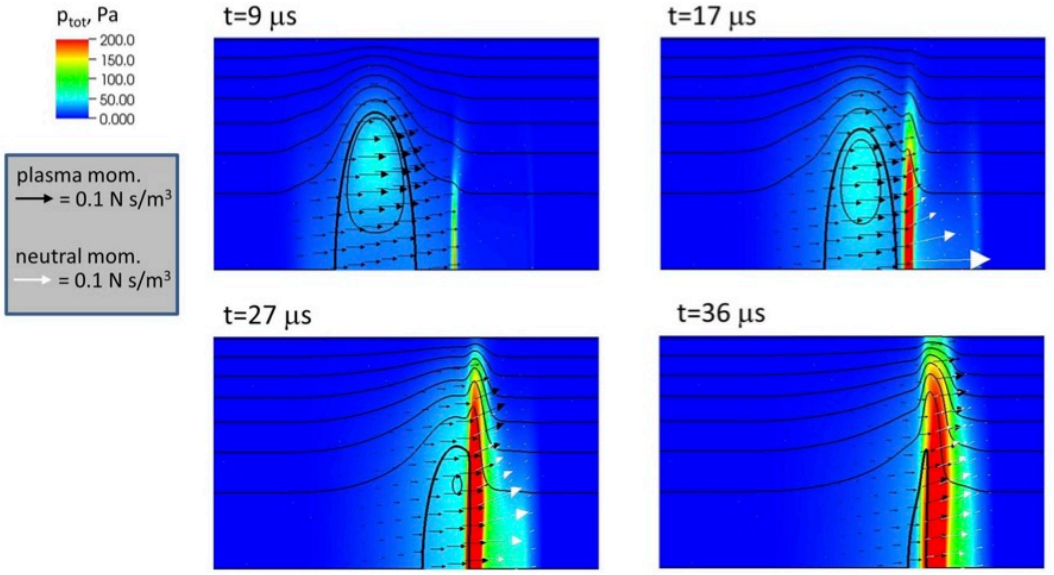

- Modeling radiation from high-Z impurities aids development of tokamak disruption mitigation techniques [Izzo, et al., PoP **15**, 056109 (2008)].

Kinetic effects from minority and majority species are included in some calculations.

- Energetic ions from beams, RF resonance, and fusion reactions have significant effects on macroscopic MHD modes.
  - Use of evolving-weight simulation particles for minority energetic particles, coupled to MHD equations through PIC-like deposition of a hot-particle pressure tensor is developed in Park, et al., PFB **4**, 2033 (1992).
  - The method was implemented in M3D-K and later in NIMROD.

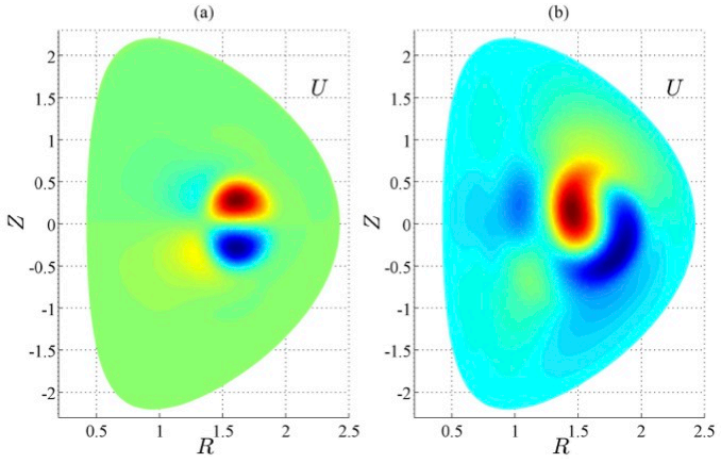

Comparison of non-resonant n=1 mode structure in NSTX without (left) and with (energetic) particle effects [Wang, et al., PoP **20**, 102506 (2013)].

- Nonlocal majority-species kinetics are important at high temperature.
  - An integro-differential approach for MHD is described in Held, et al., PoP **8**, 1171 (2001) and in Held, et al., PoP **11**, 2419 (2004).
  - Formulation of closures based on simultaneous solution of drift-kinetic equations is presented in Ramos, PoP **17**, 082502 (2010) and Ramos, PoP **18**, 102506 (2011). Implementations for NIMROD (Held) and for M3D-C1 (Lyons) are being tested.

Numerical methods for MFE MHD computations address stiffness and anisotropy.

- Temporal scales vary widely in high-performance experiments.
  - Global Alfvén-wave propagation times (τ_A) are of order 0.1-1 μs.
  - Global resistive diffusion times (τ_r) are of order 1-10 s.
  - Magnetic island development can be very slow with growth times up to 1/10 of τ_r.
- Effective time-advance methods are a focus of numerical development.
  - Implicit and semi-implicit methods are applied.
  - Some computations solve reduced models that eliminate the fastest MHD dynamics analytically.
- Extreme anisotropy with respect to the evolving direction of **B**(**x**) is another major consideration.
  - Several codes (NIMROD, M3D-C1, HiFi, JOREK, Psi-Tet) use high-order finite element methods, which helps resolve anisotropy.
  - Another approach tailors numerical heat flux densities for anisotropy [Günter et al., JCP **226**, 2306 (2007)].
- MFE codes are not designed for shock capturing.

Methods for marching nonlinear calculations in time include a range of implicitness.

- Early developments [Jardin, JCP **29**, 101 (1978); Aydemir and Barnes, JCP **59**, 108 (1985)] treat the fast wave implicitly in analogy to computation for nearly incompressible fluids.
- The quasi-implicit method of the original M3D code applies implicit fast-wave computation with a potential representation [Park, et al., NF **30**, 2413 (1990)].
- Adaptation of semi-implicit methods from weather modeling stabilizes all MHD waves without a full implicit treatment [Harned and Kerner JCP **60**, 62 (1985); Schnack, et al. JCP **70**, 330 (1987); Lerbinger and Luciani, JCP **97**, 444 (1991)]. Currently used in DEBS, XTOR (MHD), NIMROD (MHD).
- M3D-C1 has a range of two-fluid options, where the implicit operator is based on linearization about each time-step [Jardin, et al., JCP **226**, 2146 (2007); Ferraro and Jardin, JCP **228**, 7742 (2009)].
- Two-fluid computations with NIMROD use an implicit leapfrog to avoid solving all fields simultaneously [Sovinec and King, JCP **229**, 5803 (2010)].
- Several codes now use nonlinear implicit solves for *implicit balance* of all fields [Chacón, et al., JCP **178**, 15 (2002); Glasser and Tang, CPC **164**, 237 (2004); Reynolds, et al., JCP **215**, 144 (2006); Chacón, PoP **15**, 056103 (2008); Lütjens and Luciani, PoP **229**, 8130 (2010)].

Many recently developed MFE MHD codes use high-order finite elements in their spatial representation.

- NIMROD combines 2D spectral elements with 1D finite Fourier series [Sovinec, et al., JCP **195**, 355 (2004)].
- The SEL and HiFi codes use spectral elements in all directions [Glasser and Tang, CPC **164**, 237 (2004); Lukin, PhD thesis, Princeton Univ. (2008)].
- The M3D-C1 code uses reduced-quintic triangles, in combination with 1D Hermite cubics, to make values and derivatives of potential fields continuous across element borders [Jardin, JCP **200**, 133 (2004)].
- The JOREK code now uses Bézier surfaces and elements with 1D finite Fourier series [Czarny and Huysmans, JCP **227**, 7423 (2008)].
- The Psi-Tet code adapts Nedelec elements from electromagnetics for a high-order representation that separates longitudinal and solenoidal parts of vector fields in tetrahedra [Hansen, PhD thesis, Univ. of Washington (2014)].

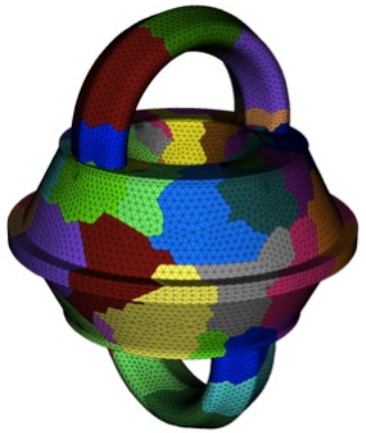

Tetrahedral mesh used for Psi-Tet simulations of the HIT-SI experiment. [Hansen, PhD thesis]

Parallel computation is essential for modeling 3D evolution.

- Fusion MHD codes use 3D domain decomposition for distributed-memory parallelism.
- Parallel computation tends to be communication-intensive.
  - Physical information propagation is fast relative to the dynamics of interest.
  - Computations with time-steps larger than global wave propagation times are common.
- Most of the wall-clock time goes to solving the algebraic systems for implicit time advances in typical MFE applications.
  - Linear systems are usually solved with Krylov-space methods (GMRES, CG, etc.).
  - Block-diagonal preconditioning with sparse direct solves, such as SuperLU_DIST [Li and Demmel, ACM TMS **29**, 110 (2003)], is applied in NIMROD and M3D-C1.
  - Nonlinearly implicit computations have been made possible with "matrix-free" Newton-Krylov solves using physics-based preconditioning [Chacón, PoP **15**, 056103 (2008)].

Discussion Points

- Some of the features of MFE MHD simulation codes may be useful for MHD power generation:
  - 3D physics
  - Two-fluid and finite-Larmor-radius modeling
  - Implicit time-stepping
  - High-order spatial representation
- Plasma/neutral modeling is relatively new but developing.
- Effect that are not modeled may be needed:
  - Shock development
  - Plasma-surface interaction
  - Other effects?